



ELSEVIER

Contents lists available at SciVerse ScienceDirect

Journal of Membrane Science

journal homepage: www.elsevier.com/locate/memsci

Pervaporation dehydration of acetic acid using polyelectrolytes complex (PEC)/11-phosphotungstic acid hydrate (PW₁₁) hybrid membrane (PEC/PW₁₁)

Jian Hua Chen^{a,*}, Jian Zhong Zheng^a, Qing Lin Liu^b, Hong Xu Guo^a, Wen Weng^a, Shun Xing Li^a

^a Department of Chemistry and Environmental Science, Zhang Zhou Normal University, Zhangzhou 363000, China

^b Department of Chemical and Biochemical Engineering, College of Chemistry & Chemical Engineering, Xiamen University, Xiamen 361005, China

ARTICLE INFO

Article history:

Received 27 July 2012

Received in revised form

7 October 2012

Accepted 17 November 2012

Available online 29 November 2012

Keywords:

Sodium alginate

Gelatin

Acetic acid

Pervaporation

ABSTRACT

Novel polyelectrolytes complex (PEC)/11-phosphotungstic acid hydrate (PW₁₁) hybrid membranes (PEC/PW₁₁) were prepared by blending sodium alginate (SA) and gelatin (GE), followed by incorporating with PW₁₁, and then crosslinking by γ -Glycidoxypropyltrimethoxysilane (GPTEOS). Structures of the membranes were characterized by X-ray diffraction (XRD), FT-IR, thermogravimetry (TG), scanning electron microscopy (SEM), atomic force microscopy (AFM) and contact angle goniometer methods. The characterization results demonstrated that the amorphous regions in the membrane and hydrophilicity of the membrane enhance with increasing PW₁₁ content; thermal stability of the membrane strengthened with the introducing of PW₁₁; PW₁₁ was homogeneously dispersed in the PEC matrix when PW₁₁ content was no higher than 9 wt%. Swelling experiments showed that the degree of swelling (DS) of the PEC/PW₁₁ hybrid membranes increased with increasing PW₁₁ content or water content in feed. Sorption experiments demonstrated that when PW₁₁ was no more than 9 wt%, both the sorption selectivity and diffusion selectivity increase with increasing PW₁₁ content, then decrease with further increasing PW₁₁ content. PEC/PW₁₁ hybrid membrane containing 9 wt% PW₁₁ exhibited the best pervaporation performance, whose averaged permeation flux was 0.440 kg/m²/h and separation factor was 144 for 90 wt% aqueous solution of acetic acid at 50 °C.

© 2012 Elsevier B.V. All rights reserved.

1. Introduction

In the past decades, membrane separation processes, for their higher selectivity, lower energy consumption, environmental friendly, moderate cost of performance and compact modular design, have offered many advantages over existing separation processes [1–4]. Pervaporation (PV) is one of membrane separation process which has a great potential for separating azeotropic mixtures, mixtures of close-boiling point and mixtures that are pressure or temperature sensitive [5–7].

Acetic acid is an important base chemical for a number of applications and ranking among the top 20 organic intermediates in the chemical industry. Acetic acid is mainly used for the production of vinyl plastics, textile finishes, latex paints, cellulose acetate, solvent to purify terephthalic acid (PTA) and acetic anhydride [8–11]. The water/acetic acid mixtures are often encountered in the preparation of several intermediates like vinyl acetate, phthalic anhydride, acetic anhydride, etc. [10]. Furthermore, the synthesis of acetic acid itself

results in the production of water as a byproduct in a number of production processes [12]. Because the relative volatility of acetic acid to water in the region of low water concentration is very close to unity [13], hence a large number of trays and a high reflux ratio are needed and so are a large column and a tremendous amount of energy to obtain glacial acetic acid, a high-purity acetic acid produced by the traditional distillation process. From an energy-saving and environmental friendly standpoint, PV can be a promising alternative to distillation for acetic acid/water separation.

Recently, polyelectrolyte–polyelectrolyte complexes (PECs), for their ease in synthesis, inherent hydrophilicity and stability at high temperatures, constitute an important family of membrane materials [14]. PECs can be prepared simply by mixing oppositely charged polyelectrolyte solution. In the PECs, electrostatic interactions constitute the main attractive forces; meanwhile, hydrogen bonding, ion dipole forces, and hydrophobic interactions may also play a significant role in determining the ultimate property [15]. PECs have been regarded as a potential practical material for several membrane processes, such as for nanofiltration membranes [16–19], membrane bioreactors [20], humidity-sensing membranes [21], proton exchange membranes [22–24] and PV membranes [25–28].

* Corresponding author. Tel.: +86 596 2591445; fax: +86 596 2520035.
E-mail address: jhchen73@126.com (J.H. Chen).

Alginate is a sodium salt of alginic acid, a naturally occurring non-toxic polysaccharide, which belongs to the carbohydrate group of polymers, found in brown algae [29]. Due to the presence of carboxyl and hydroxyl groups on the main chains, sodium alginate (SA) is one of most used hydrophilic membrane materials [30–40]. However, a very high hydrophilicity of sodium alginate leads to a significant swelling of the membrane in aqueous solution, followed by a remarkable decline of selectivity and mechanical strength. To overcome these drawbacks, several methods such as blending and filling [33–36], have been carried out to modify the NaAlg membranes for the PV dehydration of dimethylformamide [33], isopropanol [35–37], 1,4-dioxane [37,38], acetic acid [39], caprolactam [40], ethanol [41], etc. Gelatin (GE), a natural protein obtained from partially hydrolyzed collagen, is regarded as an attractive green polymer [42]. Due to its high hydrophilicity and good film forming property, GE has been utilized directly to prepare the active layer of the composite membrane [43].

In the light of the above remark, we tried to develop novel PV membranes of polyelectrolyte complexes using SA (polyanion) and GE (polycation) as matrix, with the intention to integrate the intrinsic chemical, physical, mechanical, and morphological properties of each polymer. 11-phosphotungstic acid hydrate $H_7PW_{11}O_{39}$ (PW_{11}), an unsaturated heteropolytungstate polyanion, exhibits high hydrophilicity and thermal stability. When the PW_{11} was incorporated into the PEC matrix, such organic and inorganic hybrid compounds may have the advantages of remaining the organic materials of great flexibility and good moldability as well as inorganic materials of high hydrophilicity and thermal stability. Thus properties of the PEC/ PW_{11} hybrid membrane can be improved. The physico-chemical properties of the PEC/ PW_{11} were characterized by XRD, FT-IR, TG, SEM, AFM and contact angle goniometer methods. The effects of the PW_{11} content as well as operation factor on the PV separation of water/acetic acid were investigated.

2. Experiment

2.1. Materials

Sodium alginate, Gelatin, γ -Glycidioxypropyltrimethoxysilane and other reagents, of analytical grade, were purchased from the Shanghai Chemical Reagent Store (Shanghai, China), and used without further purification.

2.2. Membrane preparation

2.2.1. PW_{11} preparation

PW_{11} was prepared according to the work of Nobuyuki [44]. In brief, dodecatungstophosphoric acid, 20 g, was dissolved in 100 ml deionized water under stirring at 85 °C. Aqueous solution of 1 M potassium hydrogencarbonate was added drop by drop to this solution under vigorous stirring until pH of the suspension becomes 5. After 30 min, the resulting mixture was filtered. The filtrate was concentrated and cooled in an ice bath. The white crystalline was dissolved in deionized water and recrystallized. The obtained PW_{11} was heated in an oven at 70 °C for 1 h.

2.2.2. PEC/ PW_{11} hybrid membranes preparation

First, SA (4.8 g) and GE (1.2 g) were dissolved in 200 ml deionized water under stirring at 90 °C. Then, various amounts of 1 M PW_{11} and 0.5 M HCl (2 ml) were added to the resulted solution under vigorous stirring for 2 h. Finally, 0.5 ml of GPTEOS was added to the solution to initiate the crosslinking reaction. The bubble-free solution was cast onto a clean glass, and then dried in an oven at

50 ± 1 °C, relative humidity of $65 \pm 2\%$ for about 2.5 h. The obtained membranes with PW_{11} content of 0, 3, 6, 9 and 12 wt% were designated as M_0 , M_1 , M_2 , M_3 and M_4 , respectively.

2.3. Membrane characterization

Crystal structure characterization of the membranes was carried out with X-ray powder diffraction (XRD, Panalytical X'pert Philip, Holland) using CuK_{α} radiation. The diffraction was operated at 40 kV and 30 mA, and the angle of diffraction was varied from 5° to 90°, using a step size of 0.0167° and a counting time of 10 s per step.

FT-IR spectra of the M_0 and M_3 membranes (4×4 cm) were scanned in the range between 4000 and 400 cm^{-1} by means of ATR-FTIR method with an accumulation of 16 scans on a Nicolet-740 (Nicolet, USA).

The surface of the PEC/ PW_{11} and the distribution of PW_{11} in the PEC matrix were investigated by field emission SEM (LEO 1530, Germany), which was operated at EHT=20 kV. Before SEM test, the samples were coated with gold by a sputter coater to improve the quality of micrograph.

The thermal stability of the M_0 and M_3 was analyzed using thermogravimetric analysis (Netzsch TG209 F1). Accurately weighted (5 mg) samples were placed into aluminum cups and heated from room temperature to 800 °C at a constant heating rate 10 °C/min under constant nitrogen purging at 20 ml/min.

Water contact angle as well as the surface energy of the membranes were measured by the pendant drop method using a contact angle meter (SL200B, SOLON TECH, Shanghai, China), equipped with a CAST2.0 software, at 25 ± 1 °C, under $70 \pm 1\%$ relative humidity condition. All reported values were the average of eight measurements taken at different location of the same membrane surface. The errors were no more than 3.5%.

A CSPM-5500 scanning probe microscope (Benyuan, China) was used to carry out the morphological characterization of the membranes, operated in tapping mode. Tapping mode cantilevers (Tap300Al, BudgetSensors) with a spring constant of 40 N/m were used throughout the imaging.

2.4. Swelling measurements and sorption experiments

The dried membranes were immersed in different concentration of water/acetic acid mixtures at 50 °C for 48 h to reach equilibrium swelling. The membranes were taken out and wiped with tissue paper to remove the surface solvent, and weighed as quickly as possible, then dipped again into the liquids. The experiments were repeated at an interval of 2 h until the weight of the sample kept approximately constant. All experiments were repeated at least for three times, and the results were averaged. The errors were no more than 2.5%. The degree of swelling (DS) was calculated by:

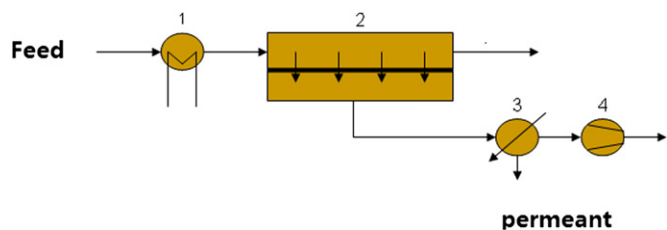
$$DS(\%) = \frac{M_W - M_D}{M_D} \times 100\% \quad (1)$$

where M_D and M_W denote the mass of the dried and swollen membranes, respectively.

For sorption experiment, the absorbed liquid was collected in a liquid nitrogen trap by desorbing the equilibrated sample in the purge-and-trap apparatus, and the concentration of the collected liquid was measured by gas chromatography. The sorption selectivity, α_s , is expressed by

$$\alpha_s = \frac{X'_W/X'_A}{X_W/X_A} \quad (2)$$

where X'_W and X'_A are the mass fraction of water and acetic acid adsorbed in the membrane; X_W and X_A are the mass fraction of water and acetic acid in the binary solution, respectively.



Scheme 1. The schematic diagram of PV: (1). Heater; (2). membrane cell; (3). liquid nitrogen trap; (4). vacuum pump.

2.5. Pervaporation measurement

The PV measurements were performed in a laboratory scale set-up as shown in Scheme 1. PV separation of water/acetic acid mixtures were performed at 30, 40, 50 60 and 70 °C, respectively. The effective membrane area was 56.06 cm². The pressure on the permeate side was maintained 600 Pa with a vacuum pump. The feed mixture was circulated between PV cell and feed tank at constant temperature. The concentrations of the feed and the permeate were measured using gas chromatography GC-4000A (Dongxi, Beijing, China) equipped with a thermal conductivity detector (TCD) and a column packed with GDX102. This chromatograph uses H₂ as the carrier gas, and H₂ flow rate was 40 ml/min. The injector temperature was 150 °C, and detector temperature was at 130 °C. The results of the PV separation of water/acetic acid mixtures were reproducible, and the errors in the PV measurements were no more than 4.0%. PV performances of the membranes were evaluated using total permeation flux (*J*) and separation factor (α_{pv}), and they can be calculated from the following equations, respectively.

$$Jp = \frac{Q}{A \times \Delta t} \quad (3)$$

$$\alpha_{pv} = \frac{Y_W/Y_A}{X_W/X_A} \quad (4)$$

where *Q* is the mass of permeate collected in the Δt time interval, and *A* is the effective membrane area, *X* and *Y* represent the mass fractions in the feed and permeate, respectively, and subscripts *W* and *A* represent water and acetic acid, respectively.

According to the solution-diffusion mechanism, diffusion selectivity, α_D , can be calculated as follows:

$$\alpha_D = \frac{\alpha_{pv}}{\alpha_s} \quad (5)$$

The value of α_{pv} focuses on the operating condition, while α_s reflects the property of the membrane materials.

3. Results and discussion

3.1. Membrane characterization

The X-ray diffraction spectra of the membranes are presented in Fig. 1. Two diffraction peaks were observed around 12.09° and 29.48° for the M₀ membrane, respectively, indicating semi-crystalline nature of the M₀ membrane. As for the PW₁₁ incorporated membranes, the peaks mentioned above became weak with increasing PW₁₁ content, indicating more amorphous regions formed in the PW₁₁ incorporated membranes. In a PV membrane, amorphous regions formed the most important passage for permeate molecules to pass through.

FT-IR analysis allowed for the qualitative and quantitative determination of the functional groups of the polymers. Fig. 2 shows the spectra of the M₀ membrane and the M₃ membrane.

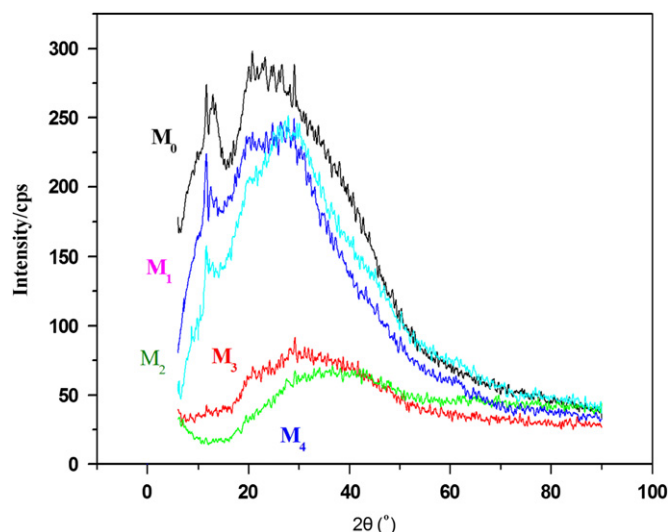


Fig. 1. XRD patterns of M₀, M₁, M₂, M₃ and M₄ membranes.

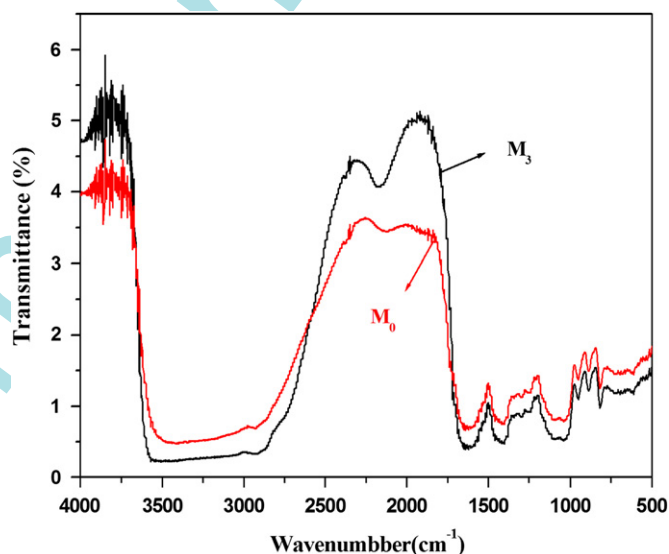


Fig. 2. FT-IR spectra of M₀ and M₃ membranes.

A characteristic strong and broad band appeared at around 3000 to 3500 cm⁻¹ for the M₀ membrane attribute to O–H stretching vibrations of the hydroxyl groups and N–H stretching vibrations of the amide groups. Comparing the spectrum of the M₃ membrane with that of the M₀ membrane, we can observe that the intensity of the characteristic band mentioned above for the M₃ membrane become stronger. Being a high hydrophilicity inorganic material, there are a great amount of hydroxyl groups on the surface of the PW₁₁. As a result, when the PW₁₁ was incorporated into the PEC matrix, the hydrophilicity of the membrane was enhanced.

Fig. 3 shows thermal properties of M₀ and M₃ membrane. As for M₀ membrane, the first weight loss stage between 33 and 103 °C is associated with the evaporation of water; the second weight loss stage between 211 and 408 °C results from the decomposition of –NH₃⁺, –COO⁻ and –OH groups; and the next one higher than 500 °C can be attributed to the main chain degradation. From Fig. 3, we also can find that thermal properties of the M₃ membrane and the M₀ membrane is similar, however, the thermal stability of the former is higher than that of the latter. This can be attributed to the high thermal stability of the PW₁₁.

When the PW_{11} was incorporated into the PEC matrix, hydroxyl groups on the surface of the PW_{11} can form hydrogen bonds with the dissociative hydroxyl groups or amine groups in the PEC matrix. Thus the thermal stability of the PEC matrix was improved.

Fig. 4 presents the SEM images of the M_0 , M_1 , M_2 , M_3 and M_4 , respectively. It is observed that the surface morphology of the membrane changes with PW_{11} content. The surface of the membrane becomes coarser with increasing PW_{11} content. The

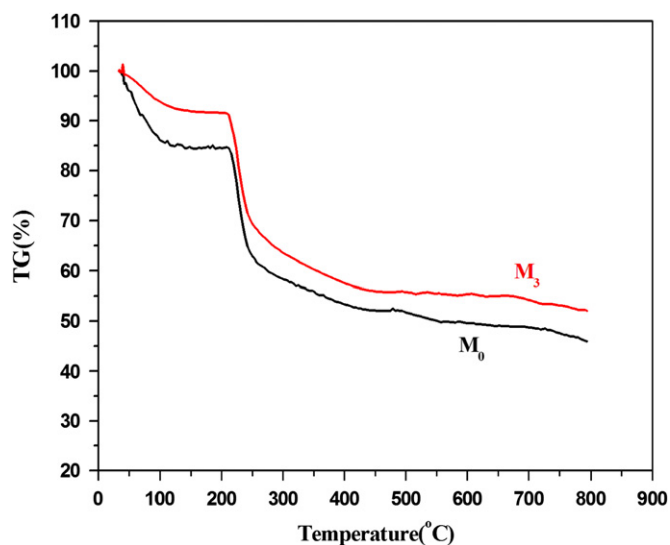


Fig. 3. TGA curves of M_0 and M_3 membranes.

surface of the M_4 membrane is the coarsest, implying agglomeration of PW_{11} in the PEC matrix.

Compared with SEM technique, AFM is able to provide the sample's tridimensional surface morphology more clear with higher resolution. As an example of images obtained by AFM, Fig. 5 shows tridimensional images of the surface of the membranes with a scope of 4000×4000 nm. Where the dark color zones represent depressions and light color regions correspond to the highest points on the surface of the membrane. The surface roughness measurements (R_a —Roughness average) calculated from the AFM images were 1.22, 1.84, 2.08, 2.55 and 5.01 nm, respectively. It indicates that the surface of the membrane becomes coarser with increasing PW_{11} content.

The water contact angle of the membrane is usually used as an indication of hydrophilicity of the membrane. The smaller the contact angle is, the more hydrophilicity of the membrane. Based on the CAST2.0 software, the water contact angle and surface energy of the membrane could be obtained. Effect of PW_{11} content on the contact angle and surface energy is presented in Fig. 6. It shows that the contact angle of the membranes steadily decrease, however, the surface energy of the membranes increase gradually with increasing PW_{11} content. The contact angle test indicated an increase in the hydrophilicity of the membrane with more PW_{11} introducing into the PEC matrix.

3.2. Swelling and sorption experiments

The pervaporation transport mechanism can be well interpreted by the solution diffusion model. Thus, preferential sorption characteristics of the membrane should be explored. Preferential sorption water in a membrane is important for PV dehydration performance since this affects the membrane permselectivity.

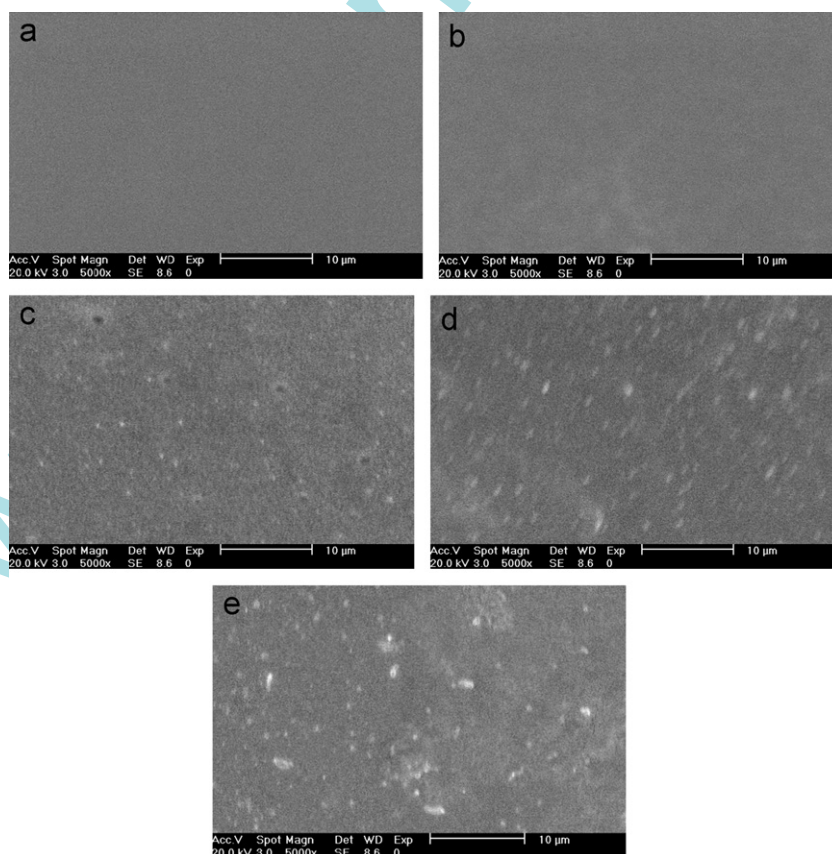


Fig. 4. SEM images of (a) M_0 ; (b) M_1 ; (c) M_2 ; (d) M_3 ; and (e) M_4 membranes.

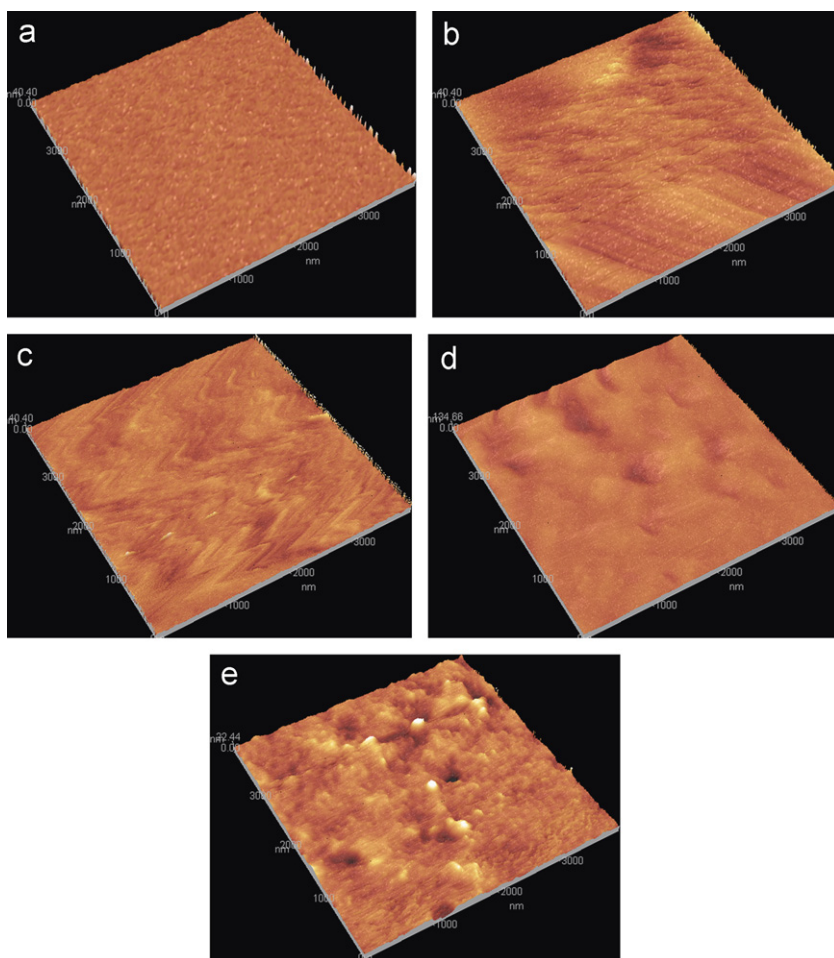


Fig. 5. AFM images of (a) M₀; (b) M₁; (c) M₂; (d) M₃; and (e) M₄ membranes.

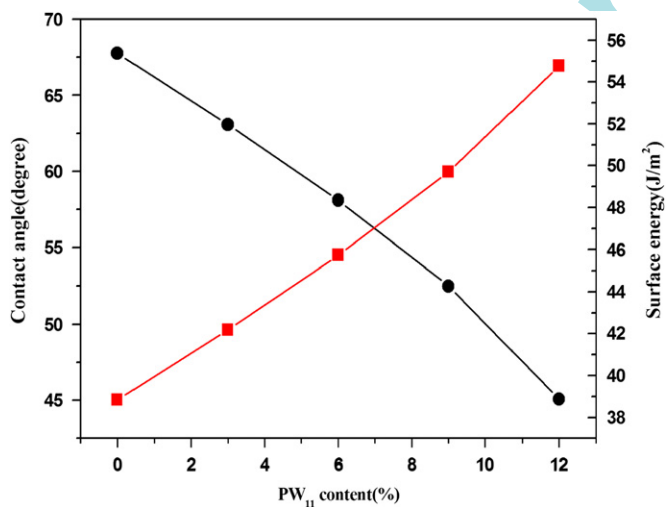


Fig. 6. Effect of PW₁₁ content on the water contact angle and the surface energy of the membrane.

Water molecules absorbed by the hydrophilic groups, such as, –NH₂, –COO[–], or –OH in the membrane results in the swelling of the membrane and assists permeates transport through the membrane. However, too much water molecules absorption in the membrane results in excessive swelling, mechanical fragility and morphological instability of the membrane. Fig. 7 presents the effect of PW₁₁ content in the membrane and acetic acid

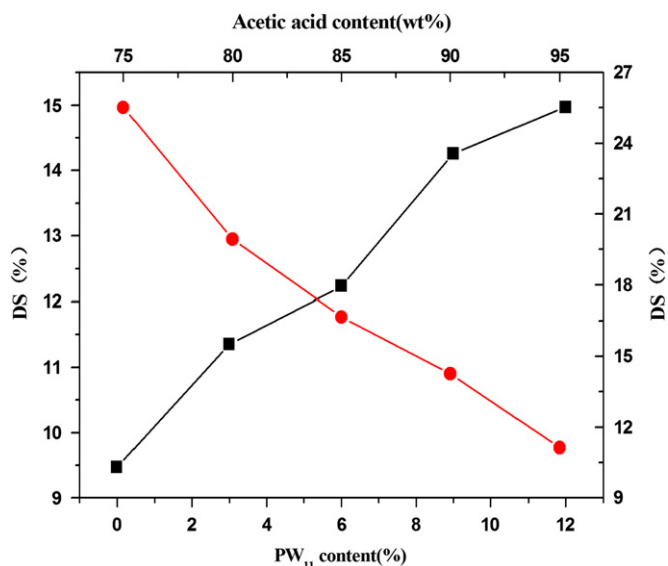


Fig. 7. Effect of PW₁₁ content (90 wt% acetic acid in feed at 50 °C) and acetic acid concentration (for M₃ membrane at 50 °C) on the DS of the membranes.

content in the feed on the DS of the membranes at 50 °C. We can observe that the DS of the membranes increase with increasing PW₁₁ content or decreasing acetic acid content. This indicated that the hydrophilicity of the membranes enhances with increasing PW₁₁ content in the membrane.

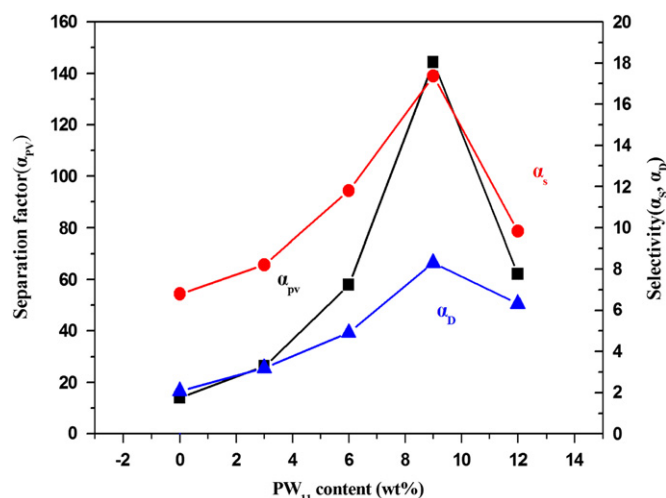


Fig. 8. Effect of PW₁₁ content on the sorption and diffusion selectivities of the membrane in PV of 90 wt% acetic acid in feed at 50 °C.

Fig. 8 presents the effect of PW₁₁ content in the membrane on the sorption selectivity and diffusion selectivity of the membranes for 90 wt% acetic acid in feed at 50 °C. It showed that both α_s and α_D increase with increasing PW₁₁ content in the membrane until the PW₁₁ content in the membrane reached 9 wt%, then decreased with further increasing PW₁₁ content. This could be attributed to the inherent hydrophilic property of the PW₁₁ and the crosslinking of the GPTEOS for PEC matrix. In preparing the hybrid membranes, GPTEOS was first hydrolyzed in the presence of an acid catalyst, leading to the formation of silanol groups. Then, the hydroxyl groups in silanol formed Si–O–N or Si–O–C bonds with the amine groups or hydroxyl groups in the PEC matrix through a dehydration reaction during the membrane drying. Also, the hydroxyl groups in the silanol can form hydrogen bonds with the dissociative hydroxyl groups or amine groups in the PEC matrix.

The introducing of the PW₁₁ enhances the hydrophilicity of the membrane, which results in an increase of the α_s of the membrane. The crosslinking of the GPTEOS for PEC matrix narrowed the passage for the permeate molecules to pass through, hence raise the α_D of the membrane. When PW₁₁ content in the membrane higher than 9 wt%, the voids originated from the phase separation of the organic phase and inorganic phase is non-selective to permeants leading to a decrease in water permselectivity. From Fig. 8, we can also observe that the value of the α_D is much lower than that of the α_s . According to the definition of separation factor (Eq. (5)), we concluded that the PV process is governed by the diffusion process.

3.3. Pervaporation experiment

3.3.1. Effect of PW₁₁ content on the PV performance

Fig. 9 presents the effect of PW₁₁ content on the PV performance in the PV separation of 90 wt% acetic acid in the feed at 50 °C. It shows that the permeation flux increases with increasing PW₁₁ content; separation selectivity first increases and reaches the maximum at 9 wt% PW₁₁ content, then decreases with further increasing PW₁₁ content. The increase in permeation flux is attributed to the increase of the amorphous region in the membrane, which favored the permeate molecules to pass through. Separation selectivity is determined by both the hydrophilicity and the size of the transport channel of the membrane. When the PW₁₁ content is less than 9 wt%, the hydrophilicity of the membrane is predominant, thus the separation selectivity of the membrane

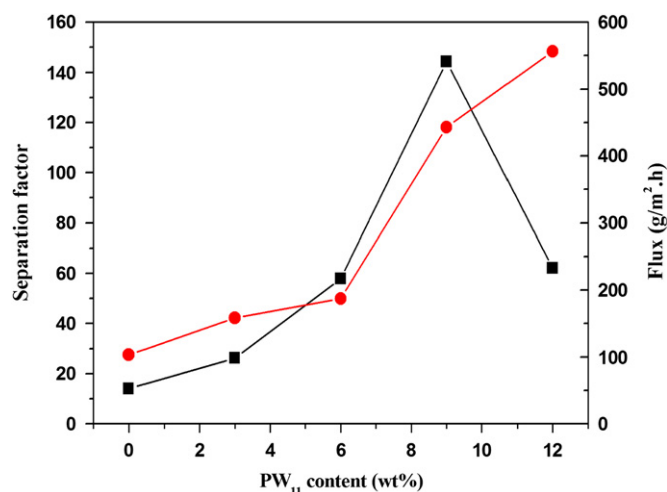


Fig. 9. Effect of PW₁₁ content on the flux and separation factor of the membranes.

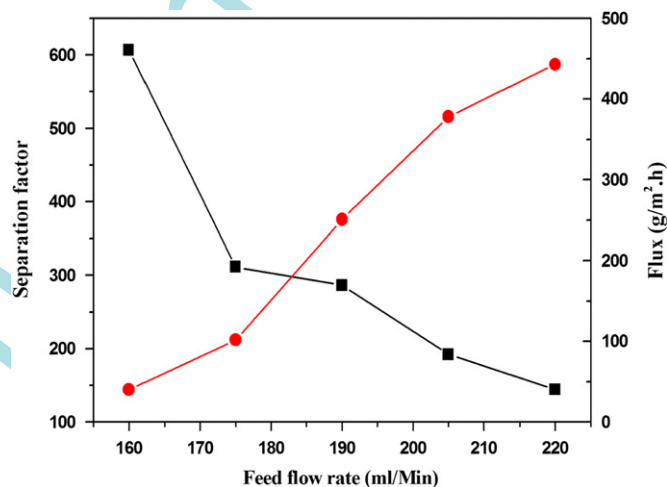


Fig. 10. Effect of feed flow rate on the flux and separation factor of the M₃ membrane.

increased with increasing PW₁₁ content. As the PW₁₁ content is higher than 9 wt%, the size of the transport channel of the membrane became predominant, which decrease the separation selectivity. Fig. 9 also indicates that the M₃ membrane shows the best PV performance. Hence, we took it for the rest of the studies.

3.3.2. Effect of feed flow rate on the PV performance

Effect of feed flow rate on the PV performance had been studied for the M₃ membrane and the results were presented in Fig. 10. It indicates that the permeation flux increases, but separation factor decreases with increasing feed flow rate from 160 to 220 ml/min. When the feed flow rate increases, the turbulence of feed solution increases, thus results in slighter concentration polarization and temperature polarization, and thinner thickness of boundary layer. Therefore, mass transfer resistance of the boundary layer on the upstream of membrane decreases and the DS of the membrane enlarges, which led to the increase of permeation flux correspondingly. Meanwhile, under the synergistic influence of the two polarizations resulting from the increasing of feed flow rate, the permeation flux of the acetic acid increases more remarkably than that of water, which lowers the separation selectivity consequently.

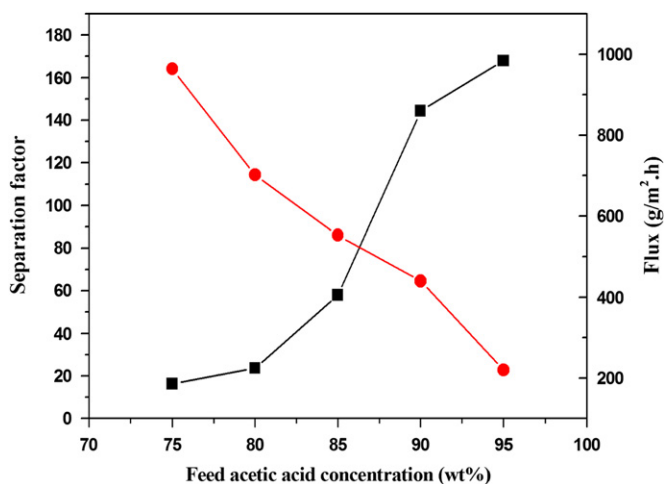


Fig. 11. Effect of feed acetic acid concentration on the flux and separation factor of the M_3 membrane at 50 °C.

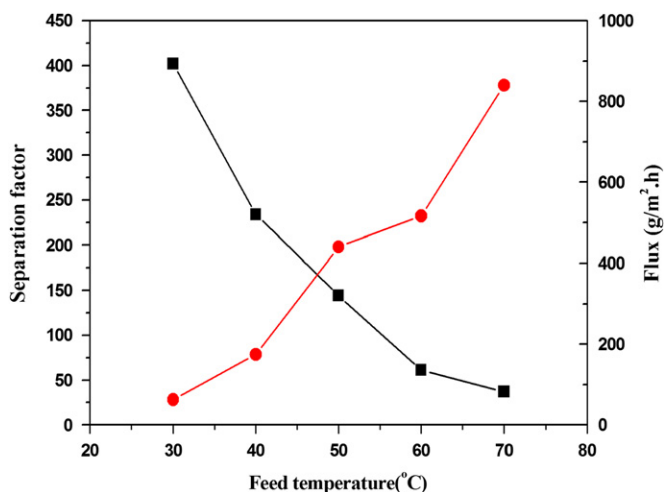


Fig. 12. Effect of feed temperature on the flux and separation factor of the M_3 membrane in PV of 90 wt% acetic acid in feed.

3.3.3. Effect of feed acetic acid concentration on the PV performance

Effect of feed acetic acid concentration, in the range of 75–95 weight%, on PV performance of the M_3 membrane has been studied. As the feed acetic acid concentration increases, the permeation flux decreases while the separation factor increases, as Fig. 11 indicated. When feed acetic acid concentration increases, the membranes become less swollen and as a result, polymer chains become less flexible and transport channel in the membrane becomes smaller, which resulting in the transport of the permeation molecules, especially for acetic acid molecule become more difficult.

3.3.4. Effect of feed temperature on the PV performance

Fig. 12 presents the PV results of an aqueous solution of 90 wt% acetic acid at 30, 40, 50, 60 and 70 °C, respectively. As expected, when the temperature was increased, the separation factor decreased, but permeation flux increased remarkably. According to the free volume theory, as the temperature increases, the frequency and amplitude of chain jumping (i.e., thermal agitation) increase, resulting in the free volumes of the membrane in the amorphous regions become larger. Increase in temperature also decreases the interaction between acetic acid and water molecules so it will be easy for both acetic acid and

water molecules to diffuse through the free volumes resulted in the decrease of the selectivity and increase of the permeation rate.

4. Conclusion

Polyelectrolytes complex nanocomposite membranes (PEC/PW₁₁) were prepared by varying the content of the PW₁₁ in the membrane and crosslinking by the GPTEOS and used for PV separation of water/acetic acid mixtures. The characterization results demonstrated that the incorporating of PW₁₁ into the PEC matrix enhanced the amorphous regions in the membrane and hydrophilicity of the membrane, hence increased the PV flux and separation selectivity. Meanwhile, the incorporating of PW₁₁ into the PEC matrix also raised thermal stability of the membrane. Sorption experiment indicated that both the sorption selectivity and diffusion selectivity of the membrane increased with increasing PW₁₁ content until the PW₁₁ content in the membrane reached 9 wt%, then both decreased with further increasing PW₁₁ content. Diffusion selectivity of the PEC/PW₁₁ membrane was less than sorption selectivity, which indicated that the PV process was dominated by the diffusion process. PEC/PW₁₁ nanocomposite membrane containing 9 wt% PW₁₁ content exhibited promising performance in PV dehydration of acetic acid.

Acknowledgments

The authors would like to thank the financial support of this work from National Natural Science Foundation of China (No. 21076174) and Fujian Education Department Foundation (type A) (No. JA 10206).

References

- [1] P.D. Chapman, T. Oliveirab, A.G. Livingstona, K. Li, Membranes for the dehydration of solvents by pervaporation, *J. Membr. Sci.* 318 (2008) 5–37.
- [2] F. Lipnizki, R.W. Field, P.K. Ten, Pervaporation-based hybrid process: a review of process design, applications and economics, *J. Membr. Sci.* 153 (1999) 183–210.
- [3] C.S. Li, X.P. Zhang, X.Z. He, et al., Design of separation process of azeotropic mixtures based on the green chemical principles, *J. Cleaner Prod.* 15 (7) (2007) 690–698.
- [4] A. Pozderović, T. Moslavac, A. Pichler, Influence of processing parameters and membrane type on permeate flux during solution concentration of different alcohols, esters, and aldehydes by reverse osmosis, *J. Food Eng.* 78 (2007) 1092–1102.
- [5] F.U. Nigiz, H. Dogan, N.D. Hilmioglu, Pervaporation of ethanol/water mixtures using clinoptilolite and 4 A filled sodium alginate membranes, *Desalination* 300 (2012) 24–31.
- [6] X.S. Wang, et al., Preparation and pervaporation characteristics of novel polyelectrolyte complex membranes containing dual anionic groups, *J. Membr. Sci.* (2012).
- [7] W. Zhang, et al., Preparation of poly(vinyl alcohol)-based membranes with controllable surface composition and bulk structures and their, *J. Membr. Sci.* (2012).
- [8] S.K. Ray, S.B. Sawant, J.B. Joshi, V.G. Pangarkar, Dehydration of acetic acid by pervaporation, *J. Membr. Sci.* 138 (1998) 1–17.
- [9] N.D. Hilmioglu, A.E. Yildirim, A.S. Sakaoglu, S. Tulbentci, Acetic acid dehydration by pervaporation, *Chem. Eng. Prog.* 40 (2001) 263–267.
- [10] K.S.V.K. Rao, B.V.K. Naidu, T.M. Aminabhavi, et al., Novel carbohydrate polymeric blend membranes in pervaporation dehydration of acetic acid, *Carbohydr. Polym.* 66 (2006) 345–351.
- [11] Tom Nora Jullok, Deforche, Patricia Luis and Bart Van der Bruggen, Sorption and diffusivity study of acetic acid and water in polymeric membranes, *Chem. Eng. Sci.* (2012) 022.
- [12] S.B. Kuila, S.K. Ray, Dehydration of acetic acid by pervaporation using filled IPN membranes, *Sep. Purif. Technol.* 81 (2011) 295–306.
- [13] J. Gmehling, U. Onken, W. Arit, Vapor–Liquid Equilibrium Data Collection, Dechema, Frankfurt/main, 1981.
- [14] Q. Zhao, J.W. Qian, Q.F. An, et al., A novel method for fabricating polyelectrolyte complex/inorganic Nanohybrid membranes with high isopropanol dehydration performance, *J. Membr. Sci.* 345 (2009) 233–241.

- [15] S.G. Kim, H.R. Ahn, K.H. Lee, Pervaporation characteristics of polyelectrolyte complex gel membranes based on two anionic polysaccharides having a chelating structure, *Curr. Appl. Phys.* 9 (2009) e42–e46.
- [16] C. Ba, D.A. Ladner, J. Economy, Using polyelectrolyte coatings to improve fouling resistance of a positively charged nanofiltration membrane, *J. Membr. Sci.* 347 (2010) 250–259.
- [17] L. Ouyang, R. Malaisamy, Merlin L. Bruening, Multilayer polyelectrolyte films as nanofiltration membranes for separating monovalent and divalent cations, *J. Membr. Sci.* 310 (2008) 76–84.
- [18] P. Ahmadiannaminia, X.F. Li, I.F.J. Vankelecom, et al., Influence of polyanion type and cationic counter ion on the SRNF performance of polyelectrolyte membranes, *J. Membr. Sci.* 403 (2012) 216–226.
- [19] P. Ahmadiannaminia, X.F. Li, I.F.J. Vankelecom, et al., Multilayered polyelectrolyte complex based solvent resistant nanofiltration membranes prepared from weak polyacids, *J. Membr. Sci.* 394 (2012) 98–106.
- [20] N. Dizge, D.Y.K. Imer, A. Karagunduz, B. Keskinler, Effects of cationic polyelectrolyte on filterability and fouling reduction of submerged membrane bioreactor (MBR), *J. Membr. Sci.* 377 (2011) 175–181.
- [21] M.S. Park, T.H. Lim, M.S. Gong, et al., A facile and simple method for the preparation of copoly(TeAMPs/VP)/silver nanocomposites for the humidity-sensing membranes, *J. Colloid Interface Sci.* 321 (2008) 60–66.
- [22] T. Zhang, W.S. He, J. Goldbach, et al., In situ proton exchange membrane fuel cell durability of poly(vinylidene fluoride)/polyelectrolyte blend Arkema M43 membrane, *J. Power Sources* 196 (2011) 1687–1693.
- [23] N. Hasanabadi, S.R. Ghaffarian, M.M.H. Sadrabadi, Magnetic field aligned nanocomposite proton exchange membranes based on sulfonated poly(ether sulfone) and Fe₂O₃ nanoparticles for direct methanol fuel cell application, *Int. J. Hydrogen Energy* 36 (2011) 15323–15332.
- [24] I. Shabania, M.M.H. Sadrabadi, V.H. Asla, M. Soleimanid, Nanofiber-based polyelectrolytes as novel membranes for fuel cell applications, *J. Membr. Sci.* 368 (2011) 233–240.
- [25] J. Xu, C.J. Gao, X.S. Feng, Thin-film-composite membranes comprising of self-assembled polyelectrolytes for separation of water from ethylene glycol by pervaporation, *J. Membr. Sci.* 352 (2010) 197–204.
- [26] X.S. Wang, et al., Preparation and pervaporation characteristics of novel polyelectrolyte complex membranes containing dual anionic groups, *J. Membr. Sci.* (2012), <http://dx.doi.org/10.1016/j.memsci.2012.04.045>.
- [27] Y.X. Liu, J.W. Qian, K. Lee, et al., The chemical crosslinking of polyelectrolyte complex colloidal particles and the pervaporation performance of their membranes, *J. Membr. Sci.* 385 (2011) 132–140.
- [28] M.H. Zhu, J.W. Qian, Q. Zhao, et al., Polyelectrolyte complex (PEC) modified by poly(vinyl alcohol) and their blend membranes for pervaporation dehydration, *J. Membr. Sci.* 378 (2011) 233–242.
- [29] R.S. Veerapur, K.B. Gudasi, T.M. Aminabhavi, Sodium alginate–magnesium aluminum silicate mixed matrix membranes for pervaporation separation of water–isopropanol mixtures, *Sep. Purif. Technol.* 59 (2008) 221–230.
- [30] S. Kalyani, B. Smithab, S. Sridhar, A. Krishnaiah, Pervaporation separation of ethanol–water mixtures through sodium alginate membranes, *Desalination* 229 (2008) 68–81.
- [31] Y.Q. Dong, L. Zhang, J.N. Shen, M.Y. Song, H.L. Chen, Preparation of poly(vinyl alcohol)- sodium alginate hollow-fiber composite membranes and pervaporation dehydration characterization of aqueous alcohol mixtures, *Desalination* 193 (2006) 202–210.
- [32] S.D. Bhat, T.M. Aminabhavi, Zeolite K-LTL-loaded sodium alginate mixed matrix membranes for pervaporation dehydration of aqueous–organic mixtures, *J. Membr. Sci.* 306 (2007) 173–185.
- [33] E.K. Solak, G. Asman, P. Camurlu, O. Sanli, Sorption, diffusion, and pervaporation characteristics of dimethylformamide/water mixtures using sodium alginate/polyvinyl pyrrolidone blend membranes, *Vacuum* 82 (2008) 579–587.
- [34] M.B. Patil, R.S. Veerapur, T.M. Aminabhavi, et al., Preparation and characterization of filled matrix membranes of sodium alginate incorporated with aluminum-containing mesoporous silica for pervaporation dehydration of alcohols, *Sep. Purif. Technol.* 54 (2007) 34–43.
- [35] S.D. Bhat, B.V.K. Naidu, T.M. Aminabhavi, et al., Mesoporous molecular sieve (MCM-41)-filled sodium alginate hybrid nanocomposite membranes for pervaporation separation of water–isopropanol mixtures, *Sep. Purif. Technol.* 49 (2006) 56–63.
- [36] M. Saraswathi, K.M. Rao, K.C. Rao, Pervaporation studies of sodium alginate (SA)/dextrin blend membranes for separation of water and isopropanol mixture, *Desalination* 269 (2011) 177–183.
- [37] S.D. Bhat, T.M. Aminabhavi, Novel sodium alginate composite membranes incorporated with SBA-15 molecular sieves for the pervaporation dehydration of aqueous mixtures of isopropanol and 1,4-dioxane at 30 °C, *Microporous Mesoporous Mater.* 91 (2006) 206–214.
- [38] B.G. Lokesh, K.S.V. Krishna Rao, P. Srinivasa Rao, et al., Novel nanocomposite membranes of sodium alginate filled with polyaniline-coated titanium dioxide for dehydration of 1,4-dioxane/water mixtures, *Desalination* 233 (2008) 166–172.
- [39] S.B. Teli, G.S. Gokavi, M. Sairam, T.M. Aminabhavi, Highly water selective silicotungstic acid (H₄SiW₁₂O₄₀) incorporated novel sodium alginate hybrid composite membranes for pervaporation dehydration of acetic acid, *Sep. Purif. Technol.* 54 (2007) 178–186.
- [40] T.R. Zhu, Y.B. Luo, P. Yu, et al., Study of pervaporation for dehydration of caprolactam through blend NaAlg–poly(vinyl pyrrolidone) membranes on PAN supports, *Sep. Purif. Technol.* 74 (2010) 242–252.
- [41] S.G. Kim, H.R. Ahn, K.H. Lee, Pervaporation characteristics of polyelectrolyte complex gel membranes based on two anionic polysaccharides having a chelating structure, *Curr. Appl. Phys.* 9 (2009) e42–e46.
- [42] J. Zhao, J. g Ma, Z.Y. Jiang, et al., Experimental and molecular simulation investigations on interfacial characteristics of gelatin/polyacrylonitrile composite pervaporation membrane, *Chem. Eng. J.* 178 (2011) 1–7.
- [43] J. Chen, X. Chen, Z.Y. Jiang, et al., Bioinspired fabrication of composite pervaporation membranes with high permeation flux and structural stability, *J. Membr. Sci.* 344 (2009) 136–143.
- [44] N. Haraguchi, Y. Okaue, T. Isobe, Y. Matsuda, Stabilization of tetravalent cerium upon coordination of unsaturated heteropolytungstate anions, *Znorg. Chem.* 33 (1994) 1015–1020.